Elastodynamic Response of a Crack Perpendicular to the Graded Interfacial Zone in Bonded Dissimilar Materials Under Antiplane Shear Impact

Sungho Kim, Hyung Jip Choi*
School of Mechanical and Automotive Engineering, Kookmin University, Seoul 136-702, Korea

A solution is given for the elastodynamic problem of a crack perpendicular to the graded interfacial zone in bonded materials under the action of antiplane shear impact. The interfacial zone is modeled as a nonhomogeneous interlayer with the power-law variations of its shear modulus and mass density between the two dissimilar, homogeneous half-planes. Laplace and Fourier integral transforms are employed to reduce the transient problem to the solution of a Cauchy-type singular integral equation in the Laplace transform domain. Via the numerical inversion of the Laplace transforms, the values of the dynamic stress intensity factors are obtained as a function of time. As a result, the influences of material and geometric parameters of the bonded media on the overshoot characteristics of the dynamic stress intensities are discussed. A comparison is also made with the corresponding elastostatic solutions, addressing the inertia effect on the dynamic load transfer to the crack tips for various combinations of the physical properties.

Key Words : Bonded Dissimilar Materials, Functionally Graded Materials, Interfacial Zone, Mode III Dynamic Stress Intensity Factors

1. Introduction

The functionally graded material features at a nonhomogeneous continuum level the smooth spatial variations of thermomechanical properties. The deliberate use of such a graded medium in the form of interfacial zone or coating can thus contribute to alleviating certain drawbacks arising from the property mismatch around sharp interfaces in the conventional, discretely layered material system (Suresh and Mortensen, 1998; Miyamoto et al., 1999). In consideration of the fail-safe concept in structural design with the graded constituent, significant progress has been made in characterizing the fatigue and fracture behavior of nonhomogeneous materials that contain crack-like flaws under various loading conditions. A number of earlier works in this area that may be of particular interest are well summarized in the review articles (Erdogan, 1998; Noda, 1999). Some additional studies that specifically deal with the elastostatic crack problems entailing the graded, nonhomogeneous properties can be found in literature (Selvadurai, 2000; Becker et al., 2001; Choi, 2001a,b,c; Choi, 2002; Dag and Erdogan, 2002; Chung et al., 2003; Bahr et al., 2003; Guo et al., 2004) and in other references cited therein. One of the most salient facets in the foregoing class of crack problems is that the near-tip stress field retains the inverse square-root singularity, together with the same angular distributions around the crack tip as those in homogeneous materials, provided the elastic properties are continuous and piecewise

* Corresponding Author,
E-mail : hjchoi@kookmin.ac.kr
TEL : +82-2-910-4682; **FAX** : +82-2-910-4839
School of Mechanical and Automotive Engineering, Kookmin University, 861-1 Chongnung-dong, Songbuk-gu, Seoul 136-702, Korea. (Manu-script **Received** January 19, 2004; **Revised** May 7, 2004)

differentiable near and at the crack tip (Eischen, 1987; Jin and Noda, 1994).

In contrast, investigations on the dynamic crack problems for the graded, nonhomogeneous materials have received rather limited attention, mainly because the corresponding elastodynamic analysis under transient loading involves more physical parameters and is more complicated when compared to its static counterpart. However, owing to the increasing applications of graded materials in critical situations where the loading may be dynamic in nature, e.g., impact or blast loading, several researchers in recent years have been engaged in developing techniques to study the cracked nonhomogeneous media subjected to time-dependent loading conditions. Jiang and Wang (2002) examined some aspects of dynamic crack propagation in a nonhomogeneous interphase, whereas Parameswaran and Shukla (1999) performed the asymptotic analysis to establish the equations for the elastic stress field around the steadily growing crack along the gradient of functionally graded materials. The evaluation of dynamic stress intensity factors for a mode III crack in a graded strip between dissimilar half-planes is due to Babaei and Lukasiewicz (1998) and the analysis of a crack in a graded coating subjected to antiplane shear impact was conducted by Shul and Lee (2002). The impact behavior of bimaterial and graded interface cracks was compared by Marur and Tippur (2000). Moreover, the torsional impact response of a penny-shaped interface crack in bonded dissimilar half-spaces with a graded interlayer was studied by Li et al. (2002). Another example of transient fracture analysis for the functionally graded material is that of an antiplane shear crack using the boundary integral equation method (Zhang et al., 2003). In particular, instead of employing certain continuous exponential or power functions to describe the material parameters of the graded media, Wang et al. (2000) and Itou (2001) simulated such materials as the sum of several sublayers with slightly different homogeneous properties in each sublayer to provide the solutions for some dynamic crack problems involving the graded properties. Most recently, Huang and Wang (2004) assigned the shear modulus and mass density that vary linearly in each sublayer and are continuous on the subinterfaces, with application to the problem of a crack in a graded interfacial zone subjected to harmonic antiplane shear loading.

In this paper, the impact response of an antiplane shear crack that is aligned perpendicular to the graded interfacial zone in bonded materials is investigated. The interfacial zone is modeled by a nonhomogeneous interlayer with the spatially varying shear modulus and mass density in terms of power functions between the two dissimilar, homogeneous half-planes. Based on the use of Laplace and Fourier integral transforms, formulation of the crack problem is reduced in the Laplace transform domain to a Cauchy-type singular integral equation. Once the integral equation is solved, the mode III stress intensity factors are defined and evaluated in the Laplace transform domain, followed by the numerical Laplace inversion to recover the time-dependence of the crack-tip response in the physical domain. As a result, a comprehensive parametric study is presented of the effects of material and geometric properties of the bonded media on the dynamic stress intensity factors, addressing the dynamic load transfer and overshoot characteristics over the corresponding elastostatic solutions.

2. Problem Statement and Basic Equations

Consider the two dissimilar, homogeneous half-planes bonded through a graded interfacial zone. As shown in Fig. 1, the half-plane on the right-hand side contains a crack of length $2c=b-a$ and location $d=(b+a)/2$ perpendicular to the interfacial zone. By modeling the interfacial zone as a nonhomogeneous interlayer of thickness h, the quantities associated with the cracked half-plane, the interlayer, and the uncracked half-plane are distinguished in order from the right-hand side and defined in the local coordinates, $(x, y)=(x_j, y)$, $j=1, 2, 3$. It is assumed that the bonded materials, which are initially at rest and stress-free, are suddenly subjected to an antiplane

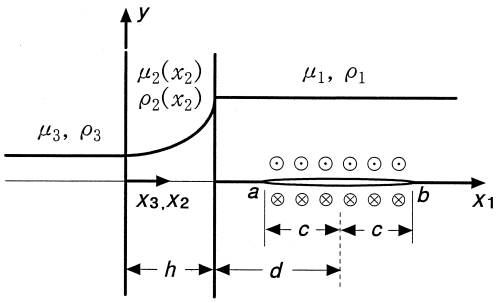

Fig. 1 Geometry, coordinate systems, and loading condition for bonded dissimilar media with a crack perpendicular to the graded interfacial zone.

shear traction applied on the crack surface. The shear moduli and mass densities of the homogeneous constituents are denoted by μ_j and ρ_j, $j=1,3$, respectively, and those of the nonhomogeneous interlayer are expressed as (Chiu and Erdogan, 1999)

$$\mu_2(x)=\mu_3(1+\alpha x)^{\beta},\ \rho_2(x)=\rho_3(1+\alpha x)^{\gamma} \quad (1)$$

where in the local coordinates $(x,y)=(x_2,y)$, the constant α and the gradient exponents β and γ are specified not only to make the transition of such properties continuous from one half-plane to the other, but to render the proposed dynamic crack problem analytically tractable, i.e.,

$$\begin{aligned}\alpha&=\frac{\sqrt{\mu_1/\mu_3}-\sqrt{\rho_1/\rho_3}}{h\sqrt{\rho_1/\rho_3}},\\ \beta&=\frac{2\ln(\mu_1/\mu_3)}{\ln(\mu_1/\mu_3)-\ln(\rho_1/\rho_3)},\\ \gamma&=\beta-2\end{aligned} \quad (2)$$

as a result, it is allowable to have the arbitrary coverage of material combinations in the bonded media with a graded, nonhomogeneous interfacial zone. It is noted that the exponential-law approximation of such properties as was assumed by Babaei and Lukasiewicz (1998) and Shul and Lee (2002) is applicable only to the special case where the mass density of the graded material varies in proportion to the shear modulus such that $\mu_1/\mu_3=\rho_1/\rho_3$, which appears to be not physically representative enough.

With $w_j(x,y,t)$, $j=1,2,3$, referring to the z-component of the displacement vector that nonvanishes under antiplane shear deformation, the corresponding stress components are given by

$$\tau_{jxz}=\mu_j\frac{\partial w_j}{\partial x},\ \tau_{jyz}=\mu_j\frac{\partial w_j}{\partial y};\ j=1,2,3 \quad (3)$$

and the equations of motion for the constituents of the bonded materials can be written as

$$\nabla^2 w_j=\frac{\rho_j}{\mu_j}\frac{\partial^2 w_j}{\partial t^2};\ j=1,3 \quad (4)$$

$$\nabla^2 w_2+\frac{\alpha\beta}{1+\alpha x}\frac{\partial w_2}{\partial x}=\frac{\rho_3}{\mu_3(1+\alpha x)^2}\frac{\partial^2 w_2}{\partial t^2} \quad (5)$$

where t is the time and ∇^2 represents the two-dimensional Laplacian operator in the variables x and y.

On account of the geometric and material symmetry about the crack plane, only the upper half of the region, $y>0$, is to be considered, subjected to the following initial conditions

$$\begin{aligned}&w_j(x_j,y,0)=0,\ \frac{\partial w_j}{\partial t}(x_j,y,0)=0;\\ &j=1,2,3,\ x_1>0,\ 0<x_2<h,\ x_3<0\end{aligned} \quad (6)$$

and the perfect bonding along the nominal interfaces between the constituents and the regularity conditions are enforced in the local coordinates as

$$\begin{aligned}&w_1(0,y,t)=w_2(h,y,t),\\ &w_2(0,y,t)=w_3(0,y,t)\end{aligned} \quad (7)$$

$$\begin{aligned}&\tau_{1xz}(0,y,t)=\tau_{2xz}(h,y,t),\\ &\tau_{2xz}(0,y,t)=\tau_{3xz}(0,y,t)\end{aligned} \quad (8)$$

$$w_1(+\infty,y,t),\ w_3(-\infty,y,t)=0 \quad (9)$$

while the mixed conditions along the crack plane, $y=0$, can be prescribed as

$$w_j(x_j,0,t)=0;\ j=2,3,\ 0<x_2<h,\ x_3<0 \quad (10)$$

$$w_1(x_1,0,t)=0;\ 0<x_1<a,\ x_1<b \quad (11)$$

$$\tau_{1yz}(x_1,0,t)=f(x_1)H(t);\ a<x_1<b \quad (12)$$

where $f(x_1)$ denotes the arbitrary crack surface traction and $H(t)$ is the Heaviside unit step function.

A pair of Laplace transform and its inverse over the time variable t is defined as (Churchill, 1981)

$$w_j^*(x_j, y, p) = \int_0^\infty w_j(x_j, y, t)\, e^{-pt} dt,$$
$$w_j(x_j, y, t) = \frac{1}{2\pi i} \int_{Br} w_j^*(x_j, y, p)\, e^{pt} dp \tag{13}$$

where p is the Laplace transform variable, Br stands for the Bromwich path of integration, and $i=(-1)^{1/2}$, so that the time-dependence in the equations of motion can be removed by the application of the Laplace transform.

Subsequently, upon applying the Fourier integral transform to the space variables in the Laplace transform domain, the general solutions for the displacement components, $w_j^*(x, y, p)$, $j=1, 2, 3$, in the local coordinates, $(x, y)=(x_j, y)$, $j=1, 2, 3$, that satisfy the regularity conditions in Eq. (9) are obtained as

$$w_1^*(x, y, p) = \frac{2}{\pi}\int_0^\infty A_1 e^{-\lambda_1 x} \sin sy\, ds + \frac{1}{2\pi}\int_{-\infty}^\infty A_2 e^{-\lambda_1 y - isx}\, ds\,; x>0 \tag{14}$$

$$w_2^*(x, y, p) = \frac{2}{\pi}(1+\alpha x)^{\frac{1-\beta}{2}}\int_0^\infty \left\{ B_1 I_v\left[\frac{s}{|\alpha|}(1+\alpha x)\right] + B_2 K_v\left[\frac{s}{|\alpha|}(1+\alpha x)\right]\right\}\sin sy\, ds \;; 0<x<h \tag{15}$$

$$w_3^*(x, y, p) = \frac{2}{\pi}\int_0^\infty C e^{\lambda_3 x} \sin sy\, ds\,; x<0 \tag{16}$$

where s is the Fourier transform variable, $A_j(s, p)$, $B_j(s, p)$, $j=1, 2$, and $C(s, p)$ are unknown functions to be determined, $I_v(\,)$ and $K_v(\,)$ are the modified Bessel functions of the first and second kind, respectively, with $\lambda_j(s, p)$, $j=1, 3$, and $v(p)$ being given by

$$\lambda_j = \sqrt{s^2 + \frac{\rho_j}{\mu_j}p^2}\,; j=1, 3,$$
$$v = \sqrt{\left(\frac{1-\beta}{2}\right)^2 + \frac{\rho_3}{\mu_3}\left(\frac{p}{\alpha}\right)^2} \tag{17}$$

and the expressions for the stress components are also obtainable in the Laplace transform domain by substituting Eqs. (14)-(16) into Eq. (3).

3. Singular Integral Equation

In solving the current crack problem, a new unknown function is introduced in the Laplace transform domain to replace the mixed conditions in Eqs. (11) and (12) as

$$\phi^*(x_1, p) = \frac{\partial}{\partial x_1} w_1^*(x_1, 0, p)\,; x_1>0 \tag{18}$$

under the single-valuedness for the displacement outside the crack line such that

$$\phi^*(x_1, p) = 0\,; 0<x_1<a,\ x_1>b \tag{19}$$

$$\int_a^b \phi^*(x_1, p)\, dx_1 = 0 \tag{20}$$

and the interface and crack surface conditions in Eqs. (7), (8), and (12) are rewritten in the Laplace transform domain as

$$w_1^*(0, y, p) = w_2^*(h, y, p),$$
$$w_2^*(0, y, p) = w_3^*(0, y, p) \tag{21}$$

$$\tau_{1xz}^*(0, y, p) = \tau_{2xz}^*(h, y, p),$$
$$\tau_{2xz}^*(0, y, p) = \tau_{3xz}^*(0, y, p) \tag{22}$$

$$\tau_{1yz}^*(x_1, 0, p) = \frac{f(x_1)}{p}\,; a<x_1<b. \tag{23}$$

It then follows from Eqs. (14), (18), and (19) that the expression for the unknown $A_2(s, p)$ is obtained as

$$A_2(s, p) = \frac{i}{s}\int_a^b \phi^*(r, p)\, e^{isr} dr \tag{24}$$

and those for the remaining unknowns, $A_1(s, p)$, $B_j(s, p)$, $j=1, 2$, and $C(s, p)$, can be determined in terms of ϕ^* by applying the interface conditions in Eqs. (21) and (22). The auxiliary function ϕ^* thus becomes the only unknown to be evaluated from the crack surface condition in Eq. (23), subjected to the compatibility condition in Eq. (20).

The traction component, τ_{1yz}^*, along the crack plane can be written by using Eqs. (3) and (14) and substituting the required expressions for $A_j(s, p)$, $j=1, 2$, such that

$$\frac{\pi}{\mu_1}\lim_{y\to+0}\tau_{1yz}^*(x, y, p) = \int_a^b \phi^*(r, p)\, dr \int_0^\infty Q(s, p)\, e^{-\lambda_1(x+r)} ds - \frac{i}{2}\int_a^b \phi^*(r, p)\, dr \int_{-\infty}^\infty R(s, p)\, e^{is(r-x)} ds \;; x>0 \tag{25}$$

with the functions $Q(s, p)$ and $R(s, p)$ given by

$$Q(s,p)=\frac{2s^2(1+ah)^{\frac{1-\beta}{2}}}{\lambda_1(f_{11}f_{22}-f_{12}f_{21})}\left\{f_{22}I_v\left[\frac{s}{|\alpha|}(1+ah)\right]-f_{21}K_v\left[\frac{s}{|\alpha|}(1+ah)\right]\right\}-\left(\frac{s}{\lambda_1}\right)^2 \tag{26}$$

$$R(s,p)=\frac{1}{s}\sqrt{s^2+\frac{\rho_1}{\mu_1}p^2} \tag{27}$$

where the contractions are made for $f_{ij}(s,p)$, $i,j=1,2$, as

$$f_{11}=\delta_1 I_v\left[\frac{s}{|\alpha|}(1+ah)\right]+\delta_2 I_{v+1}\left[\frac{s}{|\alpha|}(1+ah)\right] \tag{28}$$

$$f_{12}=\delta_1 K_v\left[\frac{s}{|\alpha|}(1+ah)\right]-\delta_2 K_{v+1}\left[\frac{s}{|\alpha|}(1+ah)\right] \tag{29}$$

$$f_{21}=\delta_3 I_v\left(\frac{s}{|\alpha|}\right)-\frac{\alpha}{|\alpha|}sI_{v+1}\left(\frac{s}{|\alpha|}\right) \tag{30}$$

$$f_{22}=\delta_3 K_v\left(\frac{s}{|\alpha|}\right)+\frac{\alpha}{|\alpha|}sK_{v+1}\left(\frac{s}{|\alpha|}\right) \tag{31}$$

in which $\delta_j(s,p)$, $j=1,2,3$, are expressed as

$$\delta_1=(1+ah)^{\frac{1-\beta}{2}}\left[\frac{\alpha(1-\beta+2v)}{2(1+ah)}+\lambda_1\right] \tag{32}$$

$$\delta_2=\frac{\alpha}{|\alpha|}s(1+ah)^{\frac{1-\beta}{2}} \tag{33}$$

$$\delta_3=\lambda_3-\frac{\alpha}{2}(1-\beta+2v). \tag{34}$$

It is noted that the integrand of the first kernel in Eq. (25) has the exponentially decaying behavior as the variable s tends to infinity, although the convergence of the related integral may be rendered relatively shower than otherwise when the variables x and r approach zero simultaneously. In addition, the function $R(s,p)$ in Eq. (27) possesses the following asymptotic property

$$\lim_{|s|\to\infty}R(s,p)=R_\infty(s)=\frac{|s|}{s} \tag{35}$$

from which it can be identified that the limiting value, $R_\infty(s)$, gives rise to the singularity the kernels in Eq. (25) may have.

As a result, after separating the singular part and applying the remaining crack surface condition in Eq. (23), an integral equation with a Cauchy singular kernel $1/(r-x)$ can be derived as

$$\int_a^b\frac{\phi^*(r,p)}{r-x}dr+\int_a^b G(x,r,p)\,\phi^*(r,p)\,dr=\frac{\pi}{\mu_1}\frac{f(x)}{p};\ a<x<b \tag{36}$$

where the function $G(x,r,p)$ is a regular kernel written in the form as

$$G(x,r,p)=\int_0^\infty[R(s,p)-R_\infty(s)]\sin s(r-x)\,ds+\int_0^\infty Q(s,p)\,e^{-\lambda_1(r+x)}ds. \tag{37}$$

Because the dominant singular kernel in the integral equation is solely attributable to the Cauchy type for $a=0$ as well as $a>0$, the near-tip stress field in the Laplace transform domain would be characterized by the inverse square-root singularity (Erdogan, 1998). The auxiliary function $\phi^*(r,p)$ is therefore expressed as (Muskhelishvili, 1953)

$$\phi^*(r,p)=\frac{g(r,p)}{\sqrt{(r-a)(b-r)}};\ a<r<b \tag{38}$$

where $g(r,p)$ is an unknown function bounded and nonzero at $r=a$ and $r=b$, and in the normalized interval

$$\begin{Bmatrix}r\\x\end{Bmatrix}=\frac{b-a}{2}\begin{Bmatrix}\eta\\\xi\end{Bmatrix}+\frac{b+a}{2};\ -1<(\xi,\eta)<1 \tag{39}$$

the solution to the integral equation can be expanded into the series of the Chebyshev polynomials of the first kind T_n as

$$\phi^*(\eta,p)=\frac{1}{p\sqrt{1-\eta^2}}\sum_{n=1}^{\infty}c_nT_n(\eta);\ |\eta|<1 \tag{40}$$

in which c_n, $n\geq 1$, are the coefficients to be calculated and this series expansion identically satisfies the compatibility condition in Eq. (20) via the orthogonality of T_n.

Upon substituting Eqs. (38)-(40) into Eq. (36), truncating the series at $n=N$, and using the properties of the Chebyshev polynomials (Abramowitz and Stegun, 1972), it can be shown that the integral equation is regularized as

$$\sum_{n=1}^{N}c_n\left[\pi U_{n-1}(\xi)+\frac{b-a}{2}\int_{-1}^{1}\frac{G(\xi,\eta,p)\,T_n(\eta)}{\sqrt{1-\eta^2}}d\eta\right]=\frac{\pi}{\mu_1}f(\xi);\ |\xi|<1 \tag{41}$$

where U_n is the Chebyshev polynomial of the second kind. To solve the above functional equations, the zeros of $T_N(\xi)$ are employed as a set of collocation points which are concentrated near the ends $\xi=\pm 1$

$$T_N(\xi_j)=0,\ \xi_j=\cos\left(\frac{\pi}{2}\frac{2j-1}{N}\right);\ j=1,2,...,N \quad (42)$$

and the integral equation can be recast into a system of linear algebraic equations for c_n, $1\leq n\leq N$, by evaluating the equations in Eq. (41) at N station points ξ_j, $1\leq j\leq N$.

Once the values of the coefficients, c_n, $1\leq n\leq N$, are determined, the integral equation in Eq. (25) provides the singular portion of the traction ahead of the crack tips. As a result, the transmission of the applied load to the crack tips and the ensuing elevation of the local stresses can be extracted by first defining and evaluating the stress intensity factors in the Laplace transform domain as

$$\begin{aligned} K^*_{\mathrm{IIIa}}(p) &= \lim_{x\to a-}\sqrt{2(a-x)}\,\tau^*_{yz}(x,0,p) \\ &= \frac{\mu_1}{p}\sqrt{\frac{b-a}{2}}\sum_{n=1}^{N}(-1)^n c_n\,;\ x<a \end{aligned} \quad (43)$$

$$\begin{aligned} K^*_{\mathrm{IIIb}}(p) &= \lim_{x\to b+}\sqrt{2(x-b)}\,\tau^*_{yz}(x,0,p) \\ &= -\frac{\mu_1}{p}\sqrt{\frac{b-a}{2}}\sum_{n=1}^{N}c_n\,;\ x>b \end{aligned} \quad (44)$$

and then the time-dependence of the stress intensification is recovered by applying the inverse Laplace transform, which can be numerically implemented by using an algorithm developed by Stehfest (1970)

$$K_{\mathrm{IIIa}}(t)\cong\frac{\ln 2}{t}\sum_{m=1}^{M}V_m K^*_{\mathrm{IIIa}}\left(\frac{m}{t}\ln 2\right);\ t>0 \quad (45)$$

$$K_{\mathrm{IIIb}}(t)\cong\frac{\ln 2}{t}\sum_{m=1}^{M}V_m K^*_{\mathrm{IIIb}}\left(\frac{m}{t}\ln 2\right);\ t>0 \quad (46)$$

where $K_{\mathrm{IIIa}}(t)$ and $K_{\mathrm{IIIb}}(t)$ represent the dynamic mode III stress intensity factors at a specific time t for the crack tips a and b, respectively, M is a positive even number, and V_m is expressed as

$$V_m=(-1)^{m+M/2}\sum_{k=(1+m)/2}^{\min(m,M/2)}\frac{k^{M/2}(2k)!}{(M/2-k)!\,k!\,(k-1)!\,(m-k)!\,(2k-m)!} \quad (47)$$

At large times, the values of the dynamic stress intensity factors would converge to those of the elastostatic solutions

$$\lim_{t\to\infty}\{K_{\mathrm{IIIa}}(t),K_{\mathrm{IIIb}}(t)\}\cong\{(K_{\mathrm{IIIa}})_{\mathrm{static}},(K_{\mathrm{IIIb}})_{\mathrm{static}}\} \quad (48)$$

and such static limits can be obtained based on the final-value theorem expressed in the form as (Churchill, 1981)

$$\{(K_{\mathrm{IIIa}})_{\mathrm{static}},(K_{\mathrm{IIIb}})_{\mathrm{static}}\}=\lim_{p\to 0+}p\{K^*_{\mathrm{IIIa}}(p),K_{\mathrm{IIIb}}{}^*(p)\} \quad (49)$$

To be mentioned is that due to the continuity of shear moduli and mass densities through the nonhomogeneous interlayer, the defined stress intensity factors are equally applicable for $a=0$ as well, which corresponds to the case of the crack-tip terminating at the nominal interface with the interlayer.

4. Numerical Results and Discussion

The variations of the dynamic stress intensity factors are presented as a function of nondimensional time $t_*=c_s t/c$ for various combinations of material (μ_3/μ_1, ρ_3/ρ_1) and geometric parameters ($h/2c$, d/c) of the problem, where $c_s=(\mu_1/\rho_1)^{1/2}$ is the shear wave velocity in the cracked constituent. The crack is assumed to be suddenly excited by the uniform antiplane traction such that $f(x_1)=-\tau_0$ in Eq. (12). In order to generate the numerical results, the series in Eq. (40) is expanded with thirty terms and the inverse Laplace transforms in Eqs. (45) and (46) are accomplished by employing fourteen terms, with the integrals in Eqs. (37) and (41) evaluated based on Gauss-Legendre and Gauss-Chebyshev quadratures, respectively (Davis and Rabinowitz, 1984). The resulting values of the dynamic stress intensity factors are normalized by $K_0=\tau_0 c^{1/2}$ and plotted in Figs. 2-9, where the corresponding elastostatic solutions from Eq. (49) are also added by the straight dotted lines.

The dynamic stress intensity factor for the case of a crack in the infinite, homogeneous medium is first obtained and compared in Fig. 2 with the closed form solution which is given in terms of an integral for the initial times (Morrissey and Geubelle, 1997)

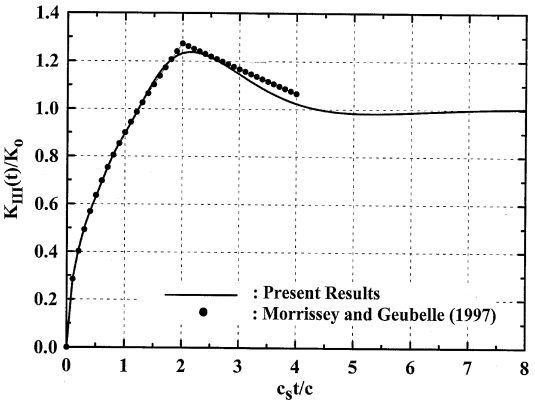

Fig. 2 Normalized dynamic stress intensity factors $K_{III}(t)/K_o$ versus nondimensional time c_st/c for homogeneous materials.

$$\frac{K_{III}(t)}{\tau_0\sqrt{c}}=\frac{4}{\pi}\left\{\sqrt{\frac{t_*}{2}}-\frac{1}{\pi}H\left(\frac{t_*}{2}-1\right)\times\int_1^{t_*/2}\left[\frac{(t_*/2-\tau)(\tau+1)}{\tau-1}\right]^{1/2}\frac{d\tau}{\tau}\right\};\quad 0\le t_*\le 4 \tag{50}$$

where it is noted that the current result is for $\mu_3/\mu_1=1.0$ and $\rho_3/\rho_1=1.001$ to avoid the division by zero in Eq. (2). A good agreement between the two solutions is observed except that the peak value is slightly different. The number of 1.238 as compared to the exact peak value $4/\pi$ from the above equation is less than 3 percent. For all practical purposes, this is within the range of deviation allowable for most engineering computations and the accuracy check may be considered satisfactory.

For the crack geometry fixed as $h/2c=0.5$ and $d/c=1.0$ and the ratio of mass density set equal to unity $\rho_3/\rho_1=1.0$, the evolution of the dynamic stress intensity factors with time at the crack tips a and b is given in Figs. 3a and 3b, respectively, for several different shear modulus ratios μ_3/μ_1. It is now appropriate to remark that in these figures and in the others that follow, the general qualitative feature of the curves is that the impact-induced stress intensity factors rise rapidly with time, reach the peaks, and then decrease in magnitude, eventually settling down to the static limits for sufficiently large times. Such a generic response is typical of the elastodynamic crack problems (Sih and Chen, 1981) that can be attributed, in this case, to the interactions between the scattered waves from the crack and the reflected waves from the nominal interfaces in the bonded media. Specifically, Figure 3a shows that the peaks are greater if the shear modulus of the uncracked constituent is less than that of the cracked constituent, i.e., $\mu_3/\mu_1<1.0$. The peak values are, however, suppressed below that of the homogeneous media when $\mu_3/\mu_1>1.0$, caused by the constraint exerted by the adjacent stiffer constituent. Further observed is that the elapsed time required for the stress intensities to arrive at the peak increases with decreasing μ_3/μ_1. Figure 3b depicts that at the crack tip b, varying the ratio

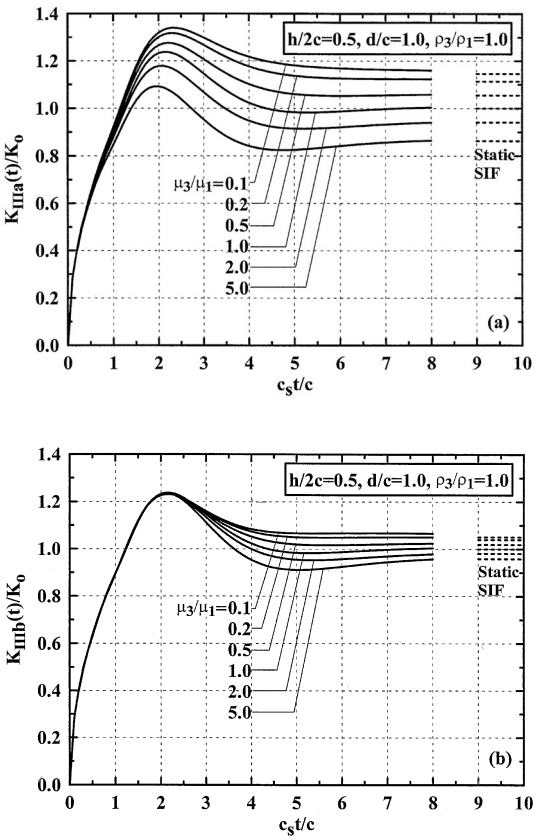

Fig. 3 Normalized dynamic stress intensity factors (a) $K_{IIIa}(t)/K_o$ and (b) $K_{IIIb}(t)/K_o$ versus nondimensional time c_st/c for different values of μ_3/μ_1 ($h/2c=0.5$, $d/c=1.0$, and $\rho_3/\rho_1=1.0$).

μ_3/μ_1 appears to hardly affect the magnitude of the overshoot in the dynamic stress intensification and the time interval in which it occurs, although the static solutions may be lowered as μ_3/μ_1 is increased. This is possibly due to the weakened influence of the waves reflected from the interface on the crack tip b that is further away from the interface, despite a wide range of variations of μ_3/μ_1.

The effect of the graded interlayer thickness depends on the shear modulus ratio, as is apparent in Figs. 4 and 5 that contain the plots of time variations of the dynamic stress intensity factors for different values of $h/2c$ and μ_3/μ_1 as well. The results in these figures assume $d/c=1.0$ and $\rho_3/\rho_1=1.0$. As expected, for the prescribed values of μ_3/μ_1, the crack tip a is shown to be sensitive to the relative interlayer thickness $h/2c$, while the peaks experienced at the crack tip b also appear to remain virtually unaffected by $h/2c$. Figure 4a exhibits that when $\mu_3/\mu_1=0.2$, the severity of the crack-tip state tends to be attenuated as $h/2c$ is increased. The increased refracted waves into the uncracked constituents and the reduced reflected waves from the interface to the crack tip for the enlarged $h/2c$ are understood to be mainly responsible for such behavior. The trend with respect to $h/2c$ thus indicates the more effective role of the graded interlayer of greater thickness in shielding the

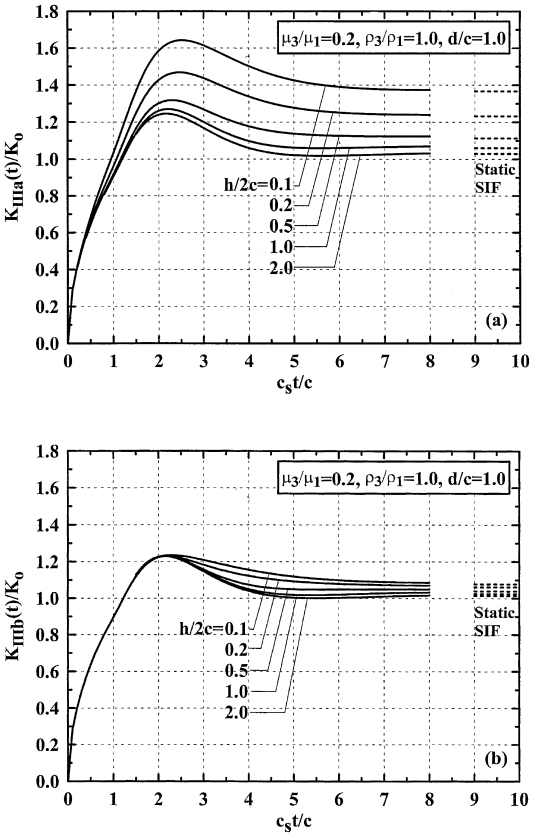

Fig. 4 Normalized dynamic stress intensity factors (a) $K_{\mathrm{IIIa}}(t)/K_o$ and (b) $K_{\mathrm{IIIb}}(t)/K_o$ versus nondimensional time $c_s t/c$ for different values of $h/2c$ ($\mu_3/\mu_1=0.2$, $\rho_3/\rho_1=1.0$, and $d/c=1.0$).

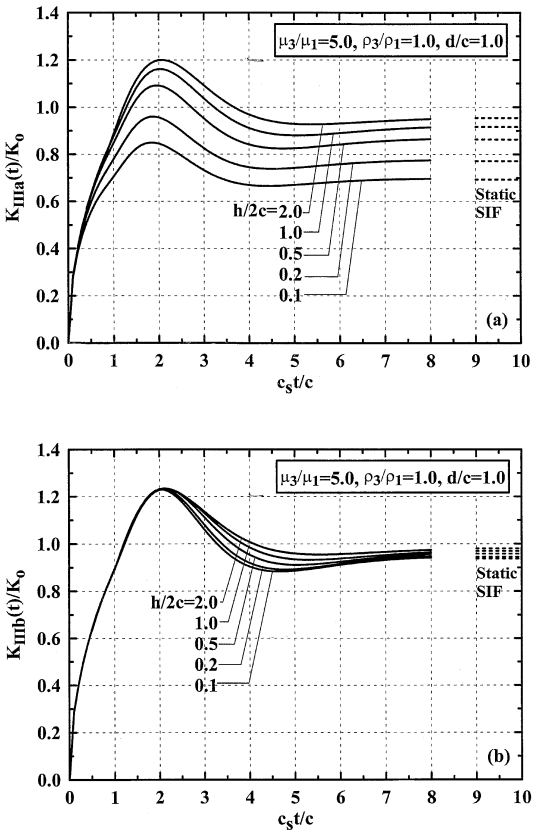

Fig. 5 Normalized dynamic stress intensity factors (a) $K_{\mathrm{IIIa}}(t)/K_o$ and (b) $K_{\mathrm{IIIb}}(t)/K_o$ versus nondimensional time $c_s t/c$ for different values of $h/2c$ ($\mu_3/\mu_1=5.0$, $\rho_3/\rho_1=1.0$, and $d/c=1.0$).

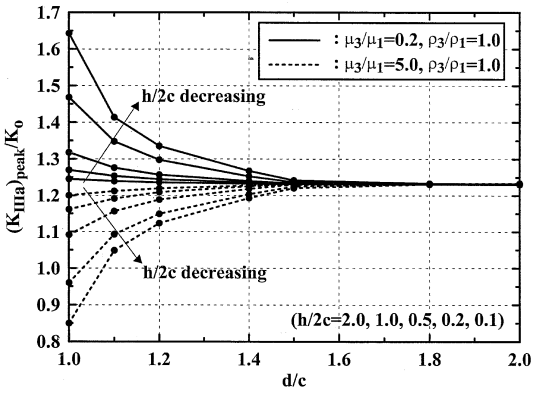

Fig. 6 Peak dynamic stress intensity factors at the crack tip a, $(K_{\mathrm{IIIa}})_{\mathrm{peak}}/K_{\mathrm{o}}$, versus crack distance d/c for different values of $h/2c$ and μ_3/μ_1 $(\rho_3/\rho_1=1.0)$.

crack that exists in the stiffer side of the bonded media. When $\mu_3/\mu_1=5.0$, the opposite response prevails so that the amplitudes of the curves in Fig. 5a drop as the interlayer is made thinner. It can then be predicted that the influence of the interlayer becomes insignificant for $h/2c>2.0$, with the solutions for the given material combinations being closely matched with that of an infinite, homogeneous plane. In addition, a careful examination of the results in Figs. 4a and 5a reveals how the interlayer thickness $h/2c$ affects the duration of the overshoot at the crack tip a. Namely, for $\mu_3/\mu_1=0.2$ $(\mu_3/\mu_1=5.0)$, the elapsed time needed to attain the maximum amplitude increases (decreases) when $h/2c$ is decreased.

To be mentioned is that increasing the crack-tip distance from the interlayer, d/c, yields a tendency, which is similar to increasing the interlayer thickness, $h/2c$. Hence, the peak values of the dynamic stress intensity factors achievable at the crack tip a after an impact are illustrated in Fig. 6 as a function of d/c for some values of $h/2c$ and μ_3/μ_1, with the mass density ratio ρ_3/ρ_1 being unity. It can be conjectured therefrom that for $h/2c>2.0$ or $d/c>1.5$, the peak values are very close to that of a crack in the infinite, homogenous medium.

The influence of the mass density ratio ρ_3/ρ_1 on the dynamic crack-tip response is next examined in Figs. 7 and 8 with two different values of μ_3/μ_1, where it is presumed that $h/2c=0.5$ and $d/c=1.0$. Figure 7a implies that when $\mu_3/\mu_1=0.2$, the near-tip region becomes less intensified as ρ_3/ρ_1 is increased. To be further observed is that the greater is the mass density ratio, the shorter is the time duration before climbing to the peak. When $\mu_3/\mu_1=5.0$, the reverse is shown in Fig. 8a, where it is interesting to note that the constraint from the nearby stiffer constituent can be counteracted by increasing ρ_3/ρ_1. For the crack tip b away from the nominal interface, Figures 7b and 8b demonstrate that the values of ρ_3/ρ_1 have almost indiscernible influence on the magnitude of the peaks and their time duration as well. Overall, the effect of the mass density ratio is less appreciable,

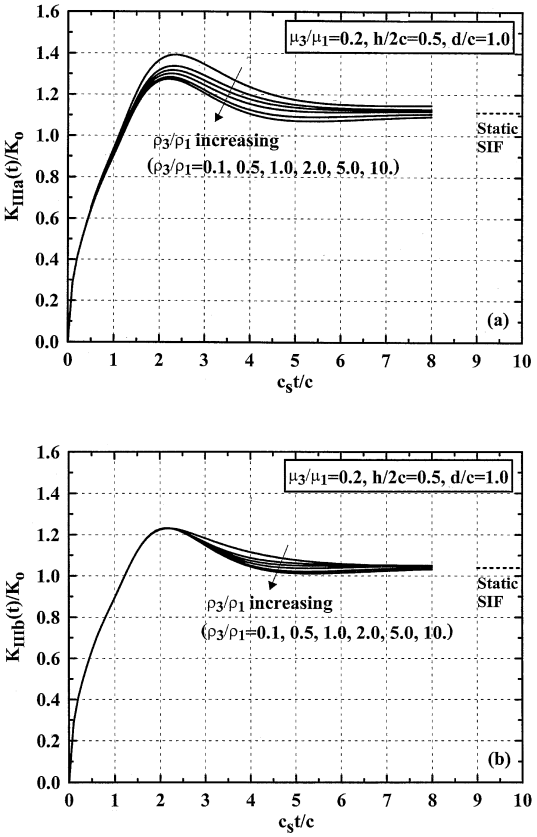

Fig. 7 Normalized dynamic stress intensity factors (a) $K_{\mathrm{IIIa}}(t)/K_{\mathrm{o}}$ and (b) $K_{\mathrm{IIIb}}(t)/K_{\mathrm{o}}$ versus nondimensional time $c_s t/c$ for different values of ρ_3/ρ_1 $(\mu_3/\mu_1=0.2,\ h/2c=0.5,$ and $d/c=1.0)$.

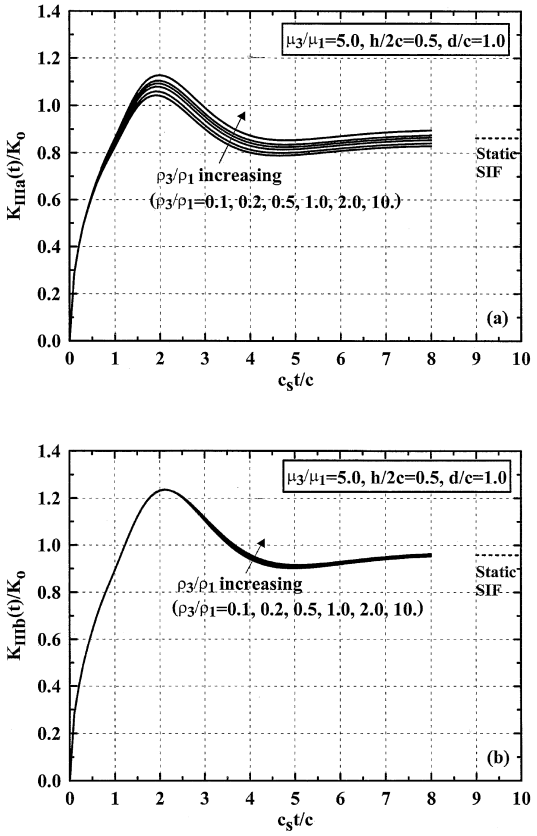

Fig. 8 Normalized dynamic stress intensity factors (a) $K_{IIIa}(t)/K_o$ and (b) $K_{IIIb}(t)/K_o$ versus nondimensional time c_st/c for different values of ρ_3/ρ_1 ($\mu_3/\mu_1=5.0$, $h/2c=0.5$, and $d/c=1.0$).

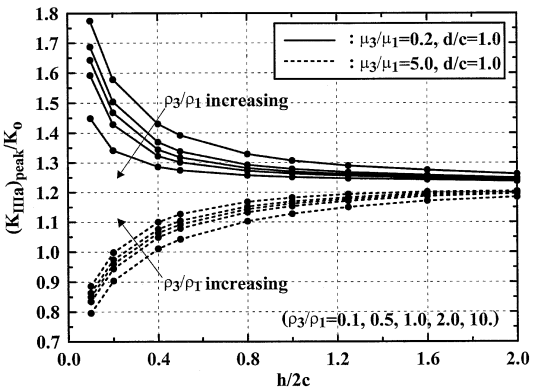

Fig. 9 Peak dynamic stress intensity factors at the crack tip a, $(K_{IIIa})_{peak}/K_o$, versus interlayer thickness $h/2c$ for different values of ρ_3/ρ_1 and μ_3/μ_1 ($d/c=1.0$).

in comparison with those of the shear modulus ratio and the interlayer thickness. With the crack located at $d/c=1.0$, additional results of the peak stress intensity factors at the crack tip a are plotted in Fig. 9 as a function of $h/2c$ for some values of ρ_3/ρ_1 and μ_3/μ_1. It can be depicted that the ratio ρ_3/ρ_1 is, in general, more influential for the smaller $h/2c$, especially when $\mu_3/\mu_1<1.0$.

As another point of interest, a comparison is made with the corresponding elastostatic solutions by extracting the ratios between the peak and static stress intensity factors, $(K_{III})_{peak}/(K_{III})_{static}$. For the crack location specified as $d/c=1.0$ and $\rho_3/\rho_1=1.0$, the results are listed in Table 1 for different values of μ_3/μ_1 and $h/2c$. Of particular interest in this table is that the ratio of the stress intensities is enlarged as μ_3/μ_1 is increased, with the implication of a more dominant effect of inertia when the uncracked constituent has the greater stiffness. Besides, when $\mu_3/\mu_1<1.0$, the inertia effect is more pronounced for the greater $h/2c$, whereas the opposite is observed for $\mu_3/\mu_1>1.0$. Tables 2 and 3 further provide the dependence of the ratio of the stress intensities on the values of ρ_3/ρ_1 and $h/2c$ for $\mu_3/\mu_1=0.2$ and 5.0, respectively, and $d/c=1.0$. In this case, it is worth noting that when the mass density of the uncracked constituent is much smaller than that of the cracked one, the generic

Table 1 Ratios of the peak dynamic stress intensity factors to the elastostatic solutions, $(K_{III})_{peak}/(K_{III})_{static}$, for different values of μ_3/μ_1 and $h/2c$ ($d/c=1.0$ and $\rho_3/\rho_1=1.0$).

$(K_{IIIa})_{peak}/(K_{IIIa})_{static}$						
μ_3/μ_1	0.1	0.2	0.5	1.0	2.0	5.0
$h/2c=0.50$	1.170	1.184	1.210	1.238	1.252	1.265
$h/2c=1.25$	1.195	1.203	1.218	1.238	1.248	1.265
$h/2c=2.00$	1.205	1.210	1.222	1.238	1.242	1.257

$(K_{IIIb})_{peak}/(K_{IIIb})_{static}$						
μ_3/μ_1	0.1	0.2	0.5	1.0	2.0	5.0
$h/2c=0.50$	1.172	1.185	1.209	1.238	1.258	1.289
$h/2c=1.25$	1.200	1.207	1.220	1.238	1.247	1.268
$h/2c=2.00$	1.208	1.213	1.222	1.238	1.241	1.257

Table 2 Ratios of the peak dynamic stress intensity factors to the elastostatic solutions, $(K_{III})_{peak}/(K_{III})_{static}$, for different values of ρ_3/ρ_1 and $h/2c$ ($\mu_3/\mu_1=0.2$ and $d/c=1.0$).

$(K_{IIIa})_{peak}/(K_{IIIa})_{static}$ ($\mu_3/\mu_1=0.2$)					
ρ_3/ρ_1	0.1	0.5	1.0	2.0	10.
$h/2c=0.50$	1.250	1.202	1.184	1.169	1.145
$h/2c=1.25$	1.231	1.210	1.203	1.198	1.190
$h/2c=2.00$	1.226	1.214	1.210	1.207	1.203

$(K_{IIIb})_{peak}/(K_{IIIb})_{static}$ ($\mu_3/\mu_1=0.2$)					
ρ_3/ρ_1	0.1	0.5	1.0	2.0	10.
$h/2c=0.50$	1.184	1.184	1.185	1.185	1.185
$h/2c=1.25$	1.206	1.207	1.207	1.207	1.207
$h/2c=2.00$	1.213	1.212	1.213	1.213	1.213

Table 3 Ratios of the peak dynamic stress intensity factors to the elastostatic solutions, $(K_{III})_{peak}/(K_{III})_{static}$, for different values of ρ_3/ρ_1 and $h/2c$ ($\mu_3/\mu_1=5.0$ and $d/c=1.0$).

$(K_{IIIa})_{peak}/(K_{IIIa})_{static}$ ($\mu_3/\mu_1=5.0$)					
ρ_3/ρ_1	0.1	0.5	1.0	2.0	10.
$h/2c=0.50$	1.208	1.250	1.265	1.279	1.306
$h/2c=1.25$	1.236	1.258	1.265	1.272	1.283
$h/2c=2.00$	1.241	1.253	1.257	1.261	1.261

$(K_{IIIb})_{peak}/(K_{IIIb})_{static}$ ($\mu_3/\mu_1=5.0$)					
ρ_3/ρ_1	0.1	0.5	1.0	2.0	10.
$h/2c=0.50$	1.290	1.290	1.289	1.289	1.289
$h/2c=1.25$	1.270	1.268	1.268	1.268	1.268
$h/2c=2.00$	1.258	1.257	1.257	1.257	1.258

trend in Table 1 with respect to $h/2c$ may not hold true at the crack tip a. It is thus observed from Table 2 that when $\mu_3/\mu_1=0.2$ and $\rho_3/\rho_1=0.1$, the effect of inertia becomes lessened for the greater $h/2c$. When $\mu_3/\mu_1=5.0$ and $\rho_3/\rho_1=0.1$, such an inertia effect becomes more notable with increasing $h/2c$ as given in Table 3. For the crack tip b that is away from the interface, however, a consistent trend exists with $h/2c$ for the given values of ρ_3/ρ_1.

5. Closing Remarks

An elastodynamic analysis has been performed to investigate the antiplane shear impact response of a crack in bonded materials in the presence of a graded interfacial zone. With the interfacial zone being modeled by a nonhomogeneous interlayer, the corresponding shear modulus and mass density were assumed to follow the power-law variations between the two dissimilar, homogeneous half-planes. The problem was formulated for the specific case of a crack located in one of the half-planes perpendicular to the interlayer and a Cauchy-type singular integral equation was derived in the Laplace transform domain. Numerical inversion of the Laplace transforms was used to evaluate the evolution of the dynamic mode III stress intensity factors with time, characterizing the influences of material and geometric parameters of the bonded media and their interactions on the magnitude and duration of the overshoot in the dynamic crack tip behavior. It was demonstrated that the values of the dynamic stress intensity factors are markedly affected by the shear modulus ratio, the interlayer thickness and the crack location as well, but are dependent to a lesser extent on the mass density ratio. In addition, the inertia effect, as measured by the ratio of the peak dynamic stress intensity factor to the elastostatic solution was addressed for various material and geometric combinations of the bonded media with the graded interlayer.

References

Abramowitz, M. and Stegun, I. A., 1972, *Handbook of Mathematical Functions*, Dover Pub., New York.

Babaei, R. and Lukasiewicz, S. A., 1998, "Dynamic Response of a Crack in a Functionally Graded Material Between Two Dissimilar Half-Planes Under Anti-Plane Shear Impact Load," *Eng. Fract. Mech.*, Vol. 60, pp. 479～487.

Bahr, H.-A., Balke, H., Fett, T., Hofinger, I., Kirchhoff, G., Munz, D., Neubrand, A., Semenov, A. S., Weiss, H.-J. and Yang, Y. Y., 2003, "Cracks in Functionally Graded Materials," *Mater. Sci. Eng. A*, Vol. 362, pp. 2～16.

Becker Jr., T. L., Cannon, R. M. and Ritchie, R. O., 2001, "Finite Crack Kinking and T-Stresses in Functionally Graded Materials," *Int.*

J. Solids Struct., Vol. 38, pp. 5545～5563.

Chiu, T.-C. and Erdogan, F., 1999, "One-Dimensional Wave Propagation in a Functionally Graded Elastic Medium," *J. Sound Vib.*, Vol. 222, pp. 453～487.

Choi, H. J., 2001a, "Mode I and Mode II Analyses of a Crack Normal to the Graded Interlayer in Bonded Materials," *KSME Int. J.*, Vol. 15, pp. 1386～1397.

Choi, H. J., 2001b, "The Problem for Bonded Half-Planes Containing a Crack at an Arbitrary Angle to the Graded Interfacial Zone," *Int. J. Solids Struct.*, Vol. 38, pp. 6559～6588.

Choi, H. J., 2001c, "Effects of Graded Layering on the Tip Behavior of a Vertical Crack in a Substrate Under Frictional Hertzian Contact," *Eng. Fract. Mech.*, Vol. 68, pp. 1033～1059.

Choi, H. J., 2002, "Driving Forces and Kinking of an Oblique Crack in Bonded Nonhomogeneous Materials," *Arch. Appl. Mech.*, Vol. 72, pp. 342～362.

Chung, Y. M., Kim, C. and Choi, H. J., 2003, "Anti-Plane Shear Behavior of an Arbitrarily Oriented Crack in Bonded Materials With a Nonhomogeneous Interfacial Zone," *KSME Int. J.*, Vol. 17, pp. 269～279.

Churchill, R. V., 1981, *Operational Mathematics*, 3rd ed., McGraw-Hill, New York.

Dag, S. and Erdogan, F., 2002, "A Surface Crack in a Graded Medium Under General Loading Conditions," *ASME J. Appl. Mech.*, Vol. 69, pp. 580～588.

Davis, P. J. and Rabinowitz, P., 1984, *Methods of Numerical Integration*, 2nd ed., Academic Press, New York.

Eischen, J. W., 1987, "Fracture of Nonhomogeneous Materials," *Int. J. Fract.*, Vol. 34, pp. 3～22.

Erdogan, F., 1998, "Crack Problems in Nonhomogeneous Materials," Cherepanov, G.P. (Ed.), *Fracture, A Topical Encyclopedia of Current Knowledge*, Krieger Pub. Company, FL, pp. 72～98.

Guo, L.-C., Wu, L. Z. and Ma, L., 2004, "The Interface Crack Problem Under a Concentrated Load for a Functionally Graded Coat-Substrate Composite System," *Comp. Struct.*, Vol. 63, pp. 397-406.

Huang, G.-Y. and Wang, Y.-S., 2004, "A New Model for Fracture Analysis of a Functionally Graded Interfacial Zone Under Harmonic Anti-Plane Loading," *Eng. Fract. Mech.*, Vol. 71, pp. 1841～1851.

Itou, S., 2001, "Transient Dynamic Stress Intensity Factors Around a Crack in a Nonhomogeneous Interfacial Layer Between Two Dissimilar Elastic Half-Planes," *Int. J. Solids Struct.*, Vol. 38, pp. 3631～3645.

Jiang, L. Y. and Wang, X. D., 2002, "On the Dynamic Crack Propagation in an Interphase With Spatially Varying Elastic Properties Under Inplane Loading," *Int. J. Fract.*, Vol. 114, pp. 225～244.

Jin, Z.-H. and Noda, N., 1994, "Crack-Tip Singular Fields in Nonhomogeneous Materials," *ASME J. Appl. Mech.*, Vol. 61, pp. 738～740.

Li, C., Duan, Z. and Zou, Z., 2002, "Torsional Impact Response of a Penny-Shaped Interface Crack in Bonded Materials With a Graded Material Interlayer," *ASME J. Appl. Mech.*, Vol. 69, pp. 303～308.

Marur, P. R. and Tippur, H. V., 2000, "Dynamic Response of Bimaterial and Graded Interface Cracks Under Impact Loading," *Int. J. Fract.*, Vol. 103, pp. 95～109.

Miyamoto, Y., Kaysser, W. A., Rabin, B. H., Kawasaki, A. and Ford, R. G. (Eds.), 1999, *Functionally Graded Materials : Design, Processing, and Applications*, Kluwer Academic Pub., MA.

Morrissey, J. W. and Geubelle, P. H., 1997, "A Numerical Scheme for Mode III Dynamic Fracture Problems," *Int. J. Num. Meth. Eng.*, Vol. 40, pp. 1181～1196.

Muskhelishvili, N. I., 1953, *Singular Integral Equations*, Noordhoff, Groningen, the Netherlands.

Noda, N., 1999, "Thermal Stresses in Functionally Graded Materials," *J. Thermal Stresses*, Vol. 22, pp. 477～512.

Parameswaran, V. and Shukla, A., 1999, "Crack-Tip Stress Fields for Dynamic Fracture in Functionally Gradient Materials," *Mech. Mater.*, Vol. 31, pp. 579～596.

Selvadurai, A. P. S., 2000, "The Penny-Shaped Crack at a Bonded Plane With Localized Elastic Non-Homogeneity," *Eur. J. Mech. A/Solids*, Vol. 19, pp. 525～534.

Shul, C. W. and Lee, K. Y., 2002, "A Subsurface Eccentric Crack in a Functionally Graded Coating Layer on the Layered Half-Space Under an Anti-Plane Shear Impact Load," *Int. J. Solids Struct.*, Vol. 39, pp. 2019～2029.

Sih, G. C. and Chen, E. P., 1981, *Mechanics of Fracture 6 : Cracks in Composite Materials*, Martinus Nijhoff Publishers, The Hague.

Stehfest, H., 1970, "Numerical Inversion of Laplace Transforms," *Commun. ACM.*, Vol. 13, pp. 47～49, 624.

Suresh, S. and Mortensen, A., 1998, *Fundamentals of Functionally Graded Materials*, The Institute of Materials, London.

Wang, B. L., Han, J. C. and Du, S. Y., 2000, "Cracks Problem for Non-Homogeneous Composite Material Subjected to Dynamic Loading," *Int. J. Solids Struct.*, Vol. 37, pp. 1251～1274.

Zhang, Ch., Savaidis, A., Savaidis, G. and Zhu, H., 2003, "Transient Dynamic Analysis of a Cracked Functionally Graded Material by a BIEM," *Comput. Mater. Sci.*, Vol. 26, pp. 167～174.